Simple estimation of synchronization threshold in ensembles of diffusively coupled chaotic systems

Andrzej Stefański,* Jerzy Wojewoda, and Tomasz Kapitaniak
Division of Dynamics, Technical University of Łódź, Stefanowskiego 1/15, 90-924 Łódź, Poland

Serhiy Yanchuk†
Weierstrass Institute for Applied Analysis and Stochastics, Mohrenstrasse 39, 10117 Berlin, Germany
(Received 22 December 2003; revised manuscript received 13 April 2004; published 30 August 2004)

In this paper, we define a simple criterion of the synchronization threshold in the set of coupled chaotic systems (flows or maps) with diagonal diffusive coupling. The condition of chaotic synchronization is determined only by two "parameters of order," i.e., the largest Lyapunov exponent and the coupling coefficient. Our approach can be applied for both regular chaotic networks and arrays or lattices of chaotic oscillators with irregular, arbitrarily assumed structure of coupling. The main idea of the synchronization stability criterion is based on linear analysis of the ensembles of simplest dynamical systems. Numerical simulations confirm that such a linear approach approximates the synchronization threshold with high precision.

DOI: 10.1103/PhysRevE.70.026217 PACS number(s): 05.45.Xt

I. INTRODUCTION

Interaction of chaotic systems has been a subject of scientific research for the past 20 years, thus the idea of synchronization has been also adopted for these systems. It has been demonstrated that two or more chaotic systems can synchronize by linking them with mutual coupling or with a common signal or signals (see, e.g., [1–14]). In the case of identical chaotic systems, i.e., the same set of ordinary different equations (ODEs) and values of the system parameters, complete synchronization can be obtained. The complete synchronization [9] takes place when all trajectories converge to the same value and remain in step during further evolution [i.e., $\lim_{t\to\infty}\|\mathbf{x}(t)-\mathbf{y}(t)\|=0$ for two arbitrarily chosen trajectories $\mathbf{x}(t)$ and $\mathbf{y}(t)$].

In particular, chaotic synchronization in networks of coupled dynamical systems has been intensively investigated in recent years. The first analytical condition for complete synchronization of the sets of symmetrically coupled identical continuous-time dynamical systems has been formulated in [4]. Next this condition has been developed for discrete-time systems [5,11]. Many approaches have been applied for describing the synchronization problem for particular coupling configurations as well as for more general cases [3,11,15–27]. Most of the existing works on networks synchronization refer to regular, symmetrical structure of coupling. However, nonsymmetrical (in particular unidirectional) and random coupling configurations have been also considered in some papers [16–19,21–27]. Especially noteworthy is a concept called the master stability function (MSF) introduced by Pecora and Carroll [21,22], which allows one to solve the network synchronization problem for any set of coupling weights and connections and any number of coupled oscillators. Other interesting solutions are the applications of graph theory to configurations of oscillators [25] and the concept of the so-called small-world networks [26,27] which connect the properties of regular and random networks.

In this paper, we present how to exploit the properties of diagonal diffusive coupling for the estimation of the network synchronization threshold. Such coupling in the ensembles of identical chaotic oscillators causes the synchronization tendency to be a product of two factors only, namely the largest Lyapunov exponent (LLE) of the node system and the effective coupling rate between them. This fact enables us to simplify theoretical analysis of the synchronization process. We introduce the concept of the *diffusive synchronization stability matrix* (DSSM) in order to investigate the stability of the synchronous regime. Our approach can be successfully applied both for flows and for maps with arbitrarily assumed structure of coupling. In Sec. II, we show how to construct the DSSM for the given case, and in Sec. III we present analytical and numerical applications of our approach for several examples of networks consisting of classical dynamical systems, i.e., Lorenz and Rössler systems, Duffing oscillator, logistic, and Henon maps.

II. SYNCHRONIZATION STABILITY ANALYSIS

Consider a set of n identical dynamical systems with diagonal diffusive coupling of arbitrary configuration between the oscillators. The equations of motion for the system are

$$\dot{\mathbf{x}}_i=\mathbf{f}(\mathbf{x}_i)+\sum_{j=1}^{n}\mathbf{D}_{ij}(\mathbf{x}_j-\mathbf{x}_i), \tag{1}$$

where $\mathbf{x}_i\in\mathbb{R}^k(k\in\mathbb{N}\geqslant 3)$, $\mathbf{f}(\mathbf{x}_i)$ is a function which governs the dynamics of each individual oscillator and $\mathbf{D}_{ij}=\mathrm{diag}[d_{ij},d_{ij},\ldots,d_{ij}]\in\mathbb{R}^k$ are diagonal coupling matrices

*Electronic address: steve@p.lodz.pl; URL:http://www.p.lodz.pl/K13
†Also at Institute of Mathematics, National Academy of Sciences of Ukraine, Tereshchenkivska 3, 01601 Kiev, Ukraine.

defining rates of coupling between each pair of the subsystems in the network ($i,j=1,2,\ldots,n$). For $\mathbf{D}_{ij}=0$ (absence of coupling), each of the subsystems given by Eq. (1) evolves on the asymptotically stable chaotic attractor $\boldsymbol{A}$. Since these oscillators are identical, it can be assumed that the solutions of equation $\dot{\mathbf{x}}_i=\mathbf{f}(\mathbf{x}_i)$ starting from different initial points of the same basin of attraction represent the set of n uncorrelated trajectories evolving on the attractor $\boldsymbol{A}$ (after a period of transient motion). Let us introduce a new variable

$$\mathbf{x}_{ij} = \mathbf{x}_i - \mathbf{x}_j \tag{2}$$

representing the *trajectories separation* between any pair of oscillators. Complete synchronization of all subsystems requires a fulfillment of the expression

$$\lim_{t\to\infty}\|\mathbf{x}_{ij}(t)\| = 0, \qquad \forall\, i,j. \tag{3}$$

As it results from the definition of Lyapunov exponents, the average distance between nearby trajectories diverges with the rate determined by LLE. On the other hand, nonzero diffusive coupling causes mutual convergence of these trajectories. In several prior works [4,11,14,16] it has been confirmed that diffusive interaction of identical strange attractors leads to the direct dependence between LLE and the coupling coefficient, which can be used for the estimation of the synchronization threshold. In our analysis, we have assumed that the analogous effect occurs in the system under consideration [Eq. (1)]. According to this approach, for sufficiently small initial *trajectories separation* distance $\mathbf{x}_{ij}(0)$ (where linear effects are dominant) the synchronization process is a product of two independent factors: (i) exponential divergence of nearby trajectories with mean rate being proportional to the positive LLE, and (ii) exponential convergence caused by introduced diffusive coupling with a rate being proportional to effective coupling.

An exact determination of the synchronization condition can be done analytically only in some simple cases of coupling configurations, e.g., symmetrical or global coupling. A more complex structure of the network requires an application of advanced mathematical and numerical techniques [16–18,21,22,25]. As follows from the *master stability function* approach [21,22] (cf. also the Appendix for details), in the case of diagonal coupling, only these two parameters of order are important for the complete synchronization. Thus, we can substitute the node by any other system characterized by the same value of LLE without the influence on the process of network synchronization and the level of synchronization threshold. This property can be used to simplify the mathematical description of complete synchronization of chaotic networks. Namely, we can reduce the system under consideration [Eq. (1)] to the linear case with $\mathbf{x}_i\in\mathbb{R}^1$ and determine the synchronization threshold on the basis of the linear stability analysis of the simplified system. In order to preserve the necessary properties, two conditions have to be fulfilled in the simplified system: (i) the substituted system in $\mathbb{R}^1$ is characterized by the same value of LLE as the original one, and (ii) original and simplified systems have identical configurations of coupling. The presented approach can be applied for continuous-time systems as well as for discrete-time systems.

TABLE I. Dynamical systems used in numerical simulations.

Dynamical system	Equations of motion	LLE$-\lambda_1$
Lorenz system	$\dot{x}=10.0(y-x)$ $\dot{y}=-xz+197.0x-y$ $\dot{z}=xy-8/3z$	1.849
Rössler system	$\dot{x}=-y-z$ $\dot{y}=x+0.15y$ $\dot{z}=0.20+z(x-10.0)$	0.085
Duffing oscillator	$\dot{x}=y$ $\dot{y}=-1.0x^3-0.10y+10\sin(t)$	0.098
Logistic map	$x_{m+1}=3.90x_m(1-x_m)$	0.485
Henon map	$x_{m+1}=1-1.40x_m^2+y_m$ $y_{m+1}=0.30x_m$	0.419

A. Continuous-time systems

In order to construct a linear model of the system [Eq. (1)] with one-dimensional nodes, we use the substitutions

$$\mathbf{f}(\mathbf{x}) = \lambda_1 x, \tag{4}$$

$$\mathbf{D}_{ij} = d_{ij}. \tag{5}$$

Note that the assumed linear system $\dot{x}=\lambda_1 x$ has no attractor, but it is not a problem here. Most important is the fact that the solution of such a linear system grows exponentially (nearby trajectories diverge with the rate λ_1), which is required by the first condition of the system transformation. Substituting Eqs. (4) and (5) into Eq. (1), we obtain a model for the network of one-dimensional systems,

$$\dot{x}_i = \lambda_1 x_i + \sum_{j=1}^{n} d_{ij}(x_j - x_i). \tag{6}$$

This simplified model can be rewritten in the vector form,

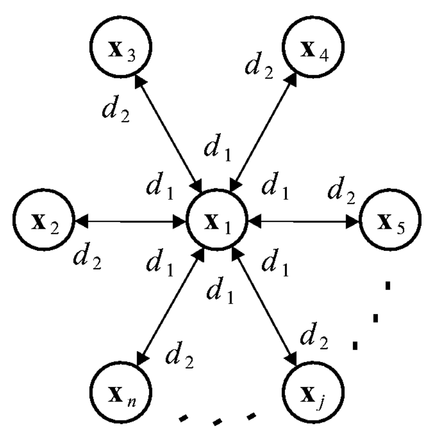

FIG. 1. Star-type configuration of coupling.

$$\dot{\mathbf{X}} = \lambda_1 \mathbf{X} + \mathbf{G}\mathbf{X}, \tag{7}$$

where $\mathbf{X}=[x_1,x_2,\ldots,x_n]^{\mathrm{T}}$, and

$$\mathbf{G} = \begin{bmatrix} -\sum_{j=1}^{n} d_{1j} & d_{12} & \cdots & d_{1n} \\ d_{21} & \ddots & & \vdots \\ \vdots & & \ddots & d_{n-1n} \\ d_{n1} & \cdots & d_{nn-1} & -\sum_{j=1}^{n} d_{nj} \end{bmatrix} \tag{8}$$

is the coupling configuration matrix (note that $d_{ii}=0$).

Let us now introduce the *trajectories separation* between arbitrarily chosen base subsystem and any other jth oscillator of the network. If we mark the base subsystem by subscript "1," we obtain

$$x_{1j} = x_1 - x_j,$$

$$x_j - x_r = x_{1r} - x_{1j} \quad (j,r = 2,3,\ldots,n). \tag{9}$$

Subtracting the remaining subsystems from the base node and applying the introduced substitutions [Eqs. (9)], we can rewrite the simplified system in $(n-1)$-dimensional form where *trajectories separation variables* are given clearly,

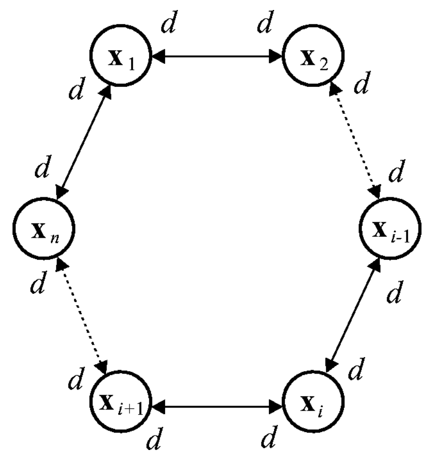

FIG. 2. Chain-type configuration of coupling.

$$\dot{\mathbf{Y}} = \mathbf{S}\mathbf{Y}, \tag{10}$$

where $\mathbf{Y}=[x_{12},x_{13},\ldots,x_{1n}]^{\mathrm{T}} \in \mathbb{R}^{n-1}$ and $(n-1)\times(n-1)$ matrix $\mathbf{S}$ assumes the form

$$\mathbf{S} = \begin{bmatrix} \lambda_1 - \left(d_{12} + \sum_{j=1}^{n} d_{2j}\right) & \cdots & d_{2k} - d_{1k} & \cdots & d_{2n} - d_{1n} \\ \vdots & \ddots & \vdots & \iddots & \vdots \\ d_{i2} - d_{12} & \cdots & \lambda_1 - \left(d_{1k} + \sum_{j=1}^{n} d_{ij}\right) & \cdots & d_{in} - d_{1n} \\ \vdots & \iddots & \vdots & \ddots & \vdots \\ d_{n2} - d_{12} & \cdots & d_{nk} - d_{1k} & \cdots & \lambda_1 - \left(d_{1n} + \sum_{j=1}^{n} d_{nj}\right) \end{bmatrix}, \tag{11}$$

where indices i and k enumerate rows and columns, respectively. The system [Eq. (10)] now incorporates only transverse dynamics to the synchronization hyperplane. Therefore, complete synchronization of all subsystems of the system [Eq. (6)] takes place if the critical point of *trajectories separation* $\mathbf{Y}=\mathbf{0}$ is a stable attractor. Such a situation occurs if real parts of all eigenvalues of the matrix Eq. (11) are negative. Thus, in agreement with the above assumptions, we can formulate the synchronization condition for the general case of a network of chaotic time-continuous systems [Eq. (1)] in the following form:

$$\mathrm{Re}(s_i) < 0, \tag{12}$$

where $s_i (i=1,2,\ldots,n-1)$ are eigenvalues of matrix $\mathbf{S}$, which we named the *diffusive synchronization stability matrix* (DSSM) due to its universal character, i.e., the form of DSSM depends only on the network coupling configuration and LLE of the dynamical system considered as a network node. The DSSM can be constructed directly from the coupling matrix [Eq. (8)] according to the model formula given by Eq. (11). In the general case, we can choose any node of the network as the base to define the DSSM, because it is of no significance for the results of synchronization stability analysis.

B. Discrete-time systems

The system analogous to Eq. (1) but consisting of n diffusively coupled identical maps is described as follows:

$$\mathbf{x}_i(m+1) = \mathbf{f}(\mathbf{x}_i(m)) + \sum_{j=1}^{n} d_{ij}\mathbf{I}_k[\mathbf{f}(\mathbf{x}_j(m)) - \mathbf{f}(\mathbf{x}_i(m))], \tag{13}$$

where $\mathbf{x}_i(m) \in \mathbb{R}^k (k \in \mathbb{N} \geqslant 1)$ and $\mathbf{I}_k$ represents a $k \times k$ unit matrix. We obtain the simplified version of Eq. (13) by applying the simplest discrete-time system,

$$x(m+1) = \exp(\lambda_1)x(m), \tag{14}$$

which fulfills the first condition of the system simplification, i.e., LLE of the map given by Eq. (14) is equal to λ_1. Using Eqs. (5) and (14), the system under consideration [Eq. (13)] is reduced to the form analogous to Eq. (6) but described by the following set of difference equations:

$$x_i(m+1) = \exp(\lambda_1)x_i(m) + \sum_{j=1}^{n} d_{ij}[\exp(\lambda_1)x_j(m) - \exp(\lambda_1)x_i(m)], \tag{15}$$

or in the vector form

$$\mathbf{X}_{m+1} = \exp(\lambda_1)[\mathbf{X}_m + G\mathbf{X}_m]. \tag{16}$$

Substituting Eq. (9) into Eq. (15) and proceeding in the way shown in Sec. II A, we formulate the difference equations of *trajectories separation* evolution,

$$\mathbf{Y}(m+1) = \mathbf{M}\mathbf{Y}(m), \tag{17}$$

and a version of DSSM for maps,

$$\mathbf{M} = \exp(\lambda_1)\begin{bmatrix} 1-\left(d_{12}+\sum_{j=1}^{n} d_{2j}\right) & \cdots & d_{2j}-d_{1j} & \cdots & d_{2n}-d_{1n} \\ \vdots & \ddots & \vdots & \iddots & \vdots \\ d_{i2}-d_{12} & \cdots & 1-\left(d_{1j}+\sum_{j=1}^{n} d_{ij}\right) & \cdots & d_{in}-d_{1n} \\ \vdots & \iddots & \vdots & \ddots & \vdots \\ d_{n2}-d_{12} & \cdots & d_{nj}-d_{1j} & \cdots & 1-\left(d_{1n}+\sum_{j=1}^{n} d_{nj}\right) \end{bmatrix}. \tag{18}$$

Hence, the synchronization threshold for the ensembles of chaotic maps with regular or random configuration of coupling is defined by the inequality

$$|\mu_i| < 1, \forall\, i, \tag{19}$$

where $\mu_i (i = 1, 2, \ldots, n-1)$ are eigenvalues of the DSSM [Eq. (18)].

III. EXAMPLES OF THE DSSM APPLICATIONS

In this section, we present some results of analytical and numerical estimation of the synchronization threshold for chosen models of chaotic networks. The analysis of synchronization stability on the basis of DSSM has been compared with results of numerical experiment for a number of arrays with regular structure of coupling and for the networks with a random coupling configuration. In numerical simulations, the examples of classical dynamical systems (flows and maps) have been applied as the network nodes. Table I presents the form of detailed equations which describe these examples with their corresponding LLEs.

A. Regular coupling configuration

In our analysis, three cases of the arrays of chaotic systems with regular structure of coupling have been considered: (i) symmetrical global coupling (each to each), (ii) star-type configuration of coupling in three versions, and (iii) chain-type (nearest-neighbor) configuration.

In the case of symmetrical global interaction, the coupling matrix [Eq. (8)] and both DSSM [Eqs. (11) and (18)] assume the forms

$$\mathbf{G} = d\begin{bmatrix} -n+1 & 1 & \cdots & 1 \\ 1 & \ddots & \ddots & \vdots \\ \vdots & \ddots & \ddots & 1 \\ 1 & \cdots & 1 & -n+1 \end{bmatrix}, \tag{20}$$

$$\mathbf{S} = \begin{bmatrix} \lambda_1 - nd & 0 & \cdots & 0 \\ 0 & \lambda_1 - nd & \cdots & 0 \\ \vdots & \vdots & \ddots & \vdots \\ 0 & 0 & \cdots & \lambda_1 - nd \end{bmatrix}, \tag{21}$$

and

$$\mathbf{M} = \exp(\lambda_1)\begin{bmatrix} 1-nd & 0 & \cdots & 0 \\ 0 & 1-nd & \cdots & 0 \\ \vdots & \vdots & \ddots & \vdots \\ 0 & 0 & \cdots & 1-nd \end{bmatrix}. \tag{22}$$

Inequalities (12) and (19) imply that complete synchronization of all network nodes occurs in the following ranges of coupling parameter:

$$d > \frac{\lambda_1}{n} \tag{23}$$

for flows and

$$\frac{1 - \exp(-\lambda_1)}{n} < d < \frac{1 + \exp(-\lambda_1)}{n} \tag{24}$$

for maps. The above conditions of synchronization stay in agreement with the results obtained earlier by means of other approaches [5,11,16].

Star-type configuration of coupling (Fig. 1) can be realized in three versions, i.e., mutual interaction (version I) and unidirectional coupling to the central node (version II) or from it (version III). If we assume the first oscillator to be the central one in a star-type configuration of coupling, then it is described by the equations

$$\begin{aligned} \dot{\mathbf{x}}_1 &= \mathbf{f}(\mathbf{x}_1) + \sum_{j=2}^{n} d_1 \mathbf{I}_k(\mathbf{x}_j - \mathbf{x}_1), \\ \dot{\mathbf{x}}_j &= \mathbf{f}(\mathbf{x}_j) + d_2 \mathbf{I}_k(\mathbf{x}_1 - \mathbf{x}_j), \end{aligned} \tag{25}$$

or

$$\begin{aligned} \mathbf{x}_1(m+1) &= \mathbf{f}(\mathbf{x}_1(m)) + \sum_{j=2}^{n} d_1 \mathbf{I}_k[\mathbf{f}(\mathbf{x}_j(m)) - \mathbf{f}(\mathbf{x}_1(m))], \\ \mathbf{x}_j(m+1) &= \mathbf{f}(\mathbf{x}_j(m)) + d_2 \mathbf{I}_k[\mathbf{f}(\mathbf{x}_1(m)) - \mathbf{f}(\mathbf{x}_j(m))], \end{aligned} \tag{26}$$

where $j = 2, 3, \langle \ldots \rangle, n$. The coupling matrix and both DSSM corresponding to the systems given by Eqs. (25) and (26) are as follows:

$$\mathbf{G} = \begin{bmatrix} (1-N)d_1 & d_1 & \cdots & d_1 \\ d_2 & -d_2 & \ddots & 0 \\ \vdots & \ddots & \ddots & \vdots \\ d_2 & 0 & \cdots & -d_2 \end{bmatrix}, \tag{27}$$

$$\mathbf{S} = \begin{bmatrix} \lambda_1 - (d_1 + d_2) & -d_1 & \cdots & -d_1 \\ -d_1 & \lambda_1 - (d_1 + d_2) & \cdots & -d_1 \\ \vdots & \vdots & \ddots & \vdots \\ -d_1 & -d_1 & \cdots & \lambda_1 - (d_1 + d_2) \end{bmatrix}, \tag{28}$$

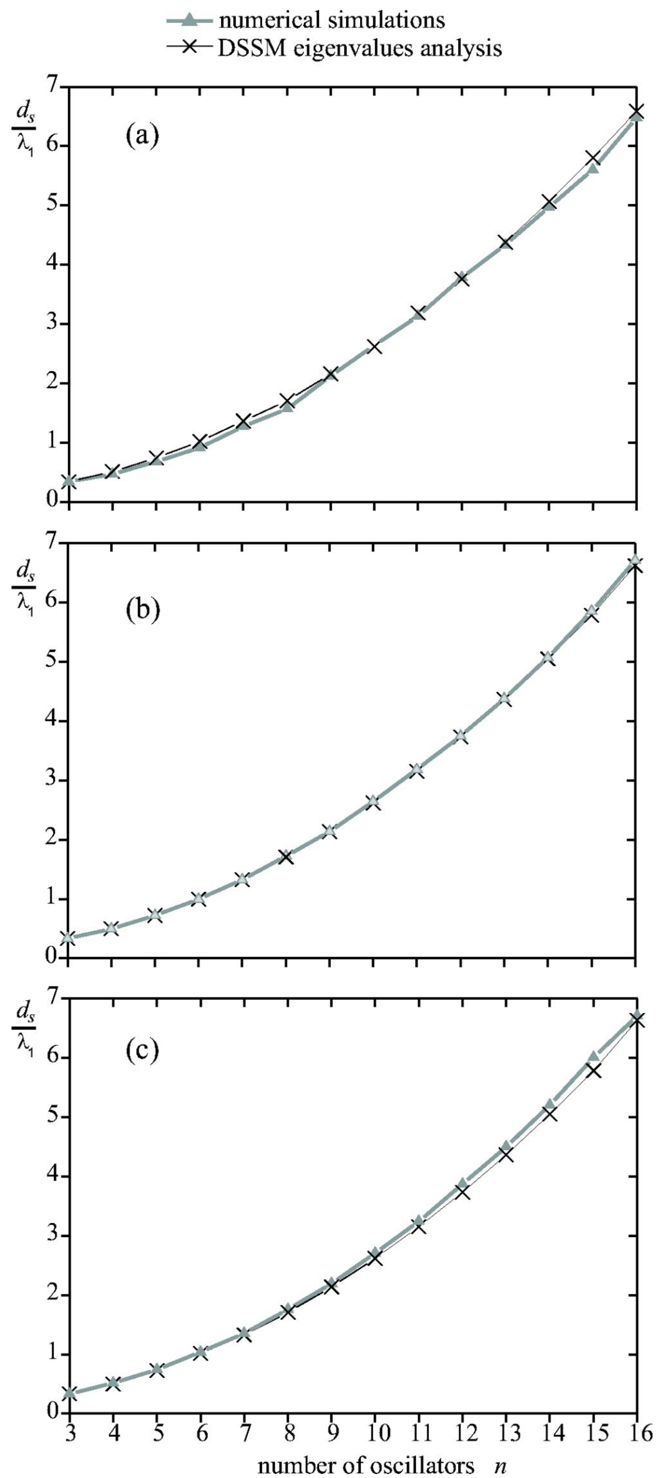

FIG. 3. The comparison of the synchronization threshold (ratio d_s/λ_1 versus the number of oscillators in chain) calculated from DSSM eigenvalues analysis and obtained from numerical investigations of chain synchronization; d_s, synchronization value of the coupling coefficient. (a) Duffing oscillators, (b) Lorenz systems, (c) Rössler systems.

$$\mathbf{M} = \exp(\lambda_1) \times \begin{bmatrix} 1-(d_1+d_2) & -d_1 & \cdots & -d_1 \\ -d_1 & 1-(d_1+d_2) & \cdots & -d_1 \\ \vdots & \vdots & \ddots & \vdots \\ -d_1 & -d_1 & \cdots & 1-(d_1+d_2) \end{bmatrix}. \tag{29}$$

The eigenvalues of both DSSM [Eqs. (28) and (29)] can be calculated analytically from the equations

$$|\mathbf{S} - s\mathbf{I}_{n-1}| = [\lambda_1 - (n-1)d_1 - d_2 - s](\lambda_1 - d_2 - s)^{n-2} = 0 \tag{30}$$

or

$$|\mathbf{M} - \mu\mathbf{I}_{n-1}| = \{\exp(\lambda_1)[1-(n-1)d_1 - d_2] - \mu\} \times [\exp(\lambda_1)(1-d_2) - \mu]^{n-2} = 0. \tag{31}$$

The synchronization threshold of time-continuous systems for the first ($d_1=d_2=d$) and the third ($d_1=0$, $d_2=d$) version of star-type coupling configurations is given by the inequality

$$d > \lambda_1. \tag{32}$$

The second version of the coupling structure ($d_1=d, d_2=0$) allows complete synchronization of periodic oscillators only, because the condition of synchronization (for flows and maps) resulting from both [Eqs. (30) and (31)] assumes the form

$$\lambda_1 < 0. \tag{33}$$

The next condition of synchronization, for the third version of maps coupled as a star ($d_1=0, d_2=d$), is given by

$$1 - \exp(-\lambda_1) < d < 1 + \exp(-\lambda_1). \tag{34}$$

The most interesting situation takes place when mutual coupling in the star-type configuration of discrete-time systems is realized ($d_1=d_2=d$). Namely, the complete synchronization is guaranteed if the coupling coefficient d fulfills the inequalities (24) and (34) simultaneously, i.e.,

$$1 - \exp(-\lambda_1) < d < \frac{1+\exp(-\lambda_1)}{n}. \tag{35}$$

Thus, in such a case the maximum number of chaotic maps which are able to synchronize is limited by the inequality

$$n < \frac{1+\exp(-\lambda_1)}{1-\exp(-\lambda_1)}. \tag{36}$$

The above presented synchronization ranges of coupling parameter [inequalities (23), (24), and (32)–(35)] which have been determined analytically can be easily confirmed in numerical simulations with an arbitrary chaotic system assumed as the network node.

The last of the above considered cases of the regular coupling configuration is the chain type, where every oscillator interacts with two nearest neighbors (Fig. 2). The equations of motion for such a case are

$$\dot{\mathbf{x}}_i = \mathbf{f}(\mathbf{x}_i) + d\mathbf{I}_k(\mathbf{x}_{i-1} - \mathbf{x}_i) + d\mathbf{I}_k(\mathbf{x}_{i+1} - \mathbf{x}_i) \tag{37}$$

and

$$\mathbf{x}_i(m+1) = \mathbf{f}[\mathbf{x}_i(m)] + d\mathbf{I}_k\{\mathbf{f}[\mathbf{x}_{i-1}(m)] - \mathbf{f}[\mathbf{x}_i(m)]\} + d\mathbf{I}_k\{\mathbf{f}[\mathbf{x}_{i+1}(m)] - \mathbf{f}[\mathbf{x}_i(m)]\}. \tag{38}$$

Hence, the coupling configuration is defined by

$$\mathbf{G} = d\begin{bmatrix} -2 & 1 & 0 & \cdots & 0 & 1 \\ 1 & -2 & 1 & \ddots & \cdots & 0 \\ 0 & 1 & \ddots & \ddots & \ddots & \vdots \\ \vdots & \ddots & \ddots & \ddots & 1 & 0 \\ 0 & \cdots & \ddots & 1 & -2 & 1 \\ 1 & 0 & \cdots & 0 & 1 & -2 \end{bmatrix}. \tag{39}$$

From the coupling matrix [Eq. (39)], we obtain the following DSSM:

$$\mathbf{S} = \begin{bmatrix} \lambda_1 - 3d & d & 0 & \cdots & \cdots & 0 & -d \\ 0 & \lambda_1 - 2d & d & \ddots & \vdots & \vdots & \vdots \\ -d & d & \lambda_1 - 2d & \ddots & 0 & \vdots & \vdots \\ \vdots & 0 & d & \ddots & d & 0 & \vdots \\ \vdots & \vdots & 0 & \ddots & \lambda_1 - 2d & d & -d \\ \vdots & \vdots & \vdots & \ddots & d & \lambda_1 - 2d & 0 \\ -d & 0 & \cdots & \cdots & 0 & d & \lambda_1 - 3d \end{bmatrix}, \tag{40}$$

$$\mathbf{M} = \exp(\lambda_1)\begin{bmatrix} 1-3d & d & 0 & \cdots & \cdots & 0 & -d \\ 0 & 1-2d & d & \ddots & \vdots & \vdots & \vdots \\ -d & d & 1-2d & \ddots & 0 & \vdots & \vdots \\ \vdots & 0 & d & \ddots & d & 0 & \vdots \\ \vdots & \vdots & 0 & \ddots & 1-2d & d & -d \\ \vdots & \vdots & \vdots & \ddots & d & 1-2d & 0 \\ -d & 0 & \cdots & \cdots & 0 & d & 1-3d \end{bmatrix}. \tag{41}$$

The synchronization threshold given by inequalities (12) and (19) has been evaluated numerically on the basis of the QR algorithm of eigenvalues calculation [28]. In Figs. 3(a)–3(c), the comparison of the results obtained from DSSM eigenvalues analysis [Eq. (40)] and from direct investigation of the synchronization process for time-continuous chaotic systems presented in Table I is illustrated. We can observe a high level of results conformity in all three examples. A similar situation is shown in Fig. 4, where the synchronization analysis of the logistic maps (from Table I) chain is presented. Also in this case the synchronization ranges of coupling coefficient determined from eigenvalues of DSSM [Eq. (41)] agree with appropriate regions obtained from numerical simulations of chain dynamics. Our analysis additionally demonstrates that for $n \geqslant 7$, the complete synchronization in the chain under consideration is impossible because for arbitrary d, the condition of synchronization [inequality (19)] is not fulfilled.

B. Random coupling configuration

The first example consists of four randomly coupled chaotic oscillators according to the scheme shown in Fig. 5. The corresponding coupling configuration matrix has the following form:

$$\mathbf{G} = d\begin{bmatrix} -3 & 1 & 2 & 0 \\ 2 & -2 & 0 & 0 \\ 1 & 0 & -1 & 0 \\ 3 & 2 & 0 & -5 \end{bmatrix}. \tag{42}$$

It is obvious that an irregular coupling configuration causes nonsymmetrical, random structure of both DSSM,

$$\mathbf{S} = \begin{bmatrix} \lambda_1-3d & -2d & 0 \\ -d & \lambda_1-3d & 0 \\ 0 & -2d & \lambda_1-4d \end{bmatrix} \tag{43}$$

and

$$\mathbf{M} = \exp(\lambda_1)\begin{bmatrix} 1-3d & -2d & 0 \\ -d & 1-3d & 0 \\ 0 & -2d & 1-4d \end{bmatrix}. \tag{44}$$

The eigenvalues of the above matrices [Eqs. (43) and (44)] can be calculated analytically as

$$s_1 = \lambda_1 - 4d, s_{2,3} = \lambda_1 - (3 \pm \sqrt{2})\, d$$

or

$$\mu_1 = \exp(\lambda_1)(1-4d),$$

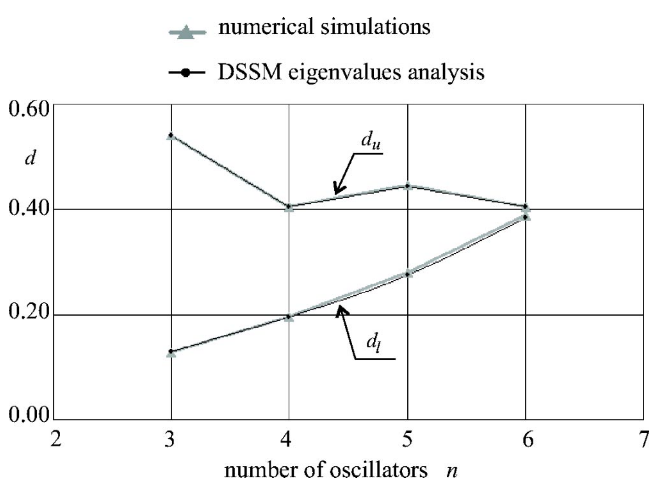

FIG. 4. The comparison of the synchronization ranges of coupling coefficient d in the chain of diffusively coupled logistic maps calculated from DSSM eigenvalues analysis and obtained from numerical simulations; d_u and d_l, upper and lower ends of the synchronization range.

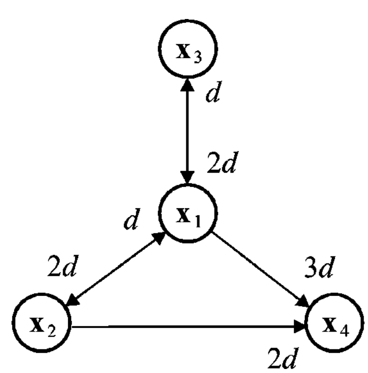

FIG. 5. Four oscillators with irregular configuration of coupling.

$$\mu_{2,3} = \exp(\lambda_1)[1 - (3 \pm \sqrt{2})d].$$

Substituting these eigenvalues into inequalities (12) and (19), we obtain the synchronization ranges of parameter d for the network shown in Fig. 5,

$$d > \frac{\lambda_1}{3 - \sqrt{2}} \tag{45}$$

for flows and

$$\frac{1 - \exp(-\lambda_1)}{3 - \sqrt{2}} < d < \frac{1 + \exp(-\lambda_1)}{3 + \sqrt{2}} \tag{46}$$

for maps. The confirmation of complete synchronization stability regions given by inequalities (45) and (46) is shown in Figs. 6(a) and 6(b), where the comparison of analytical results with numerical simulations is presented. As the examples of nodes in the considered network (Fig. 5), the Rössler oscillator and Henon map have been used.

The last example is a set of ten identical time-continuous systems (Duffing oscillators) with randomly assumed coupling structure represented by the matrix

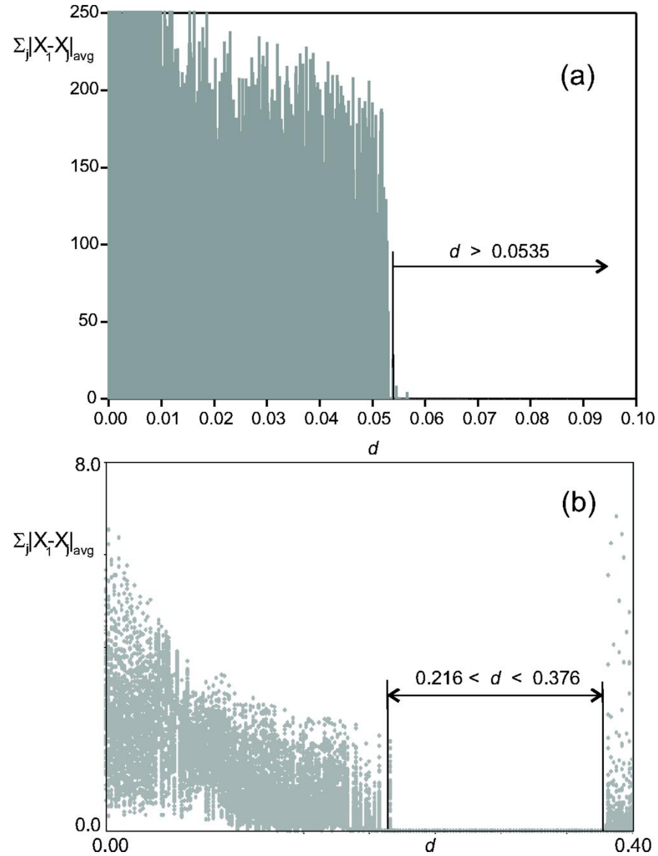

FIG. 6. Bifurcation diagrams (the sum of average *trajectories separation* vs coupling coefficient) representing the comparison of the synchronization ranges in the ensembles of dynamical systems [(a) set of Rössler systems, (b) set of logistic maps] with the scheme of connections shown in Fig. 5. The ranges obtained analytically according to Eqs. (45) and (46) are marked and described in black.

$$\mathbf{G} = d\begin{bmatrix} -17 & 0 & 2 & 4 & 0 & 0 & 7 & 0 & 4 & 0 \\ 0 & -17 & 2 & 8 & 0 & 1 & 0 & 0 & 0 & 6 \\ 0 & 0 & -17 & 1 & 5 & 0 & 7 & 4 & 0 & 0 \\ 9 & 2 & 0 & -21 & 0 & 3 & 5 & 1 & 0 & 1 \\ 4 & 6 & 7 & 1 & -23 & 0 & 0 & 3 & 2 & 0 \\ 5 & 0 & 0 & 0 & 10 & -19 & 3 & 0 & 0 & 1 \\ 0 & 1 & 3 & 10 & 2 & 0 & -18 & 0 & 2 & 0 \\ 0 & 4 & 3 & 0 & 0 & 5 & 7 & -19 & 0 & 0 \\ 1 & 0 & 0 & 2 & 0 & 0 & 0 & 10 & -13 & 0 \\ 7 & 4 & 0 & 0 & 10 & 2 & 0 & 1 & 2 & -26 \end{bmatrix}. \tag{47}$$

The DSSM resulting from the coupling matrix [Eq. (47)] is as follows:

$$\mathbf{S} = \lambda_1 \mathbf{I}_9 + d \begin{bmatrix} -17 & 0 & 4 & 0 & 1 & -7 & 0 & -4 & 6 \\ 0 & -19 & -2 & 5 & 0 & 0 & 4 & -4 & 0 \\ 2 & -2 & -25 & 0 & 3 & -2 & 1 & -4 & 1 \\ 6 & 5 & -3 & -23 & 0 & -7 & 3 & -2 & 0 \\ 0 & -2 & -4 & 10 & -19 & -4 & 0 & -4 & 1 \\ 1 & 1 & 6 & 2 & 0 & -25 & 0 & -2 & 0 \\ 4 & 1 & -4 & 0 & 5 & 0 & -19 & -4 & 0 \\ 0 & -2 & -2 & 0 & 0 & -7 & 10 & -17 & 0 \\ 4 & -2 & -4 & 10 & 2 & -7 & 1 & -2 & -26 \end{bmatrix}. \tag{48}$$

In Figs. 7(a) and 7(b), numerically calculated real parts of the eigenvalues of DSSM [Eq. (48), Fig. 7(b)] and the corresponding *trajectories separation* bifurcation diagram [Fig. 7(a)] drawn as a function of coupling parameter d are shown. Comparing both diagrams, we can see that according to inequality (12), the synchronization appears [*trajectories separation* tends to zero in Fig. 7(a)] if all real parts of DSSM eigenvalues become negative. Thus, even in such a case of a larger number of oscillators with completely irregular coupling structure, calculation of the synchronization threshold by means of the DSSM method is a simple task.

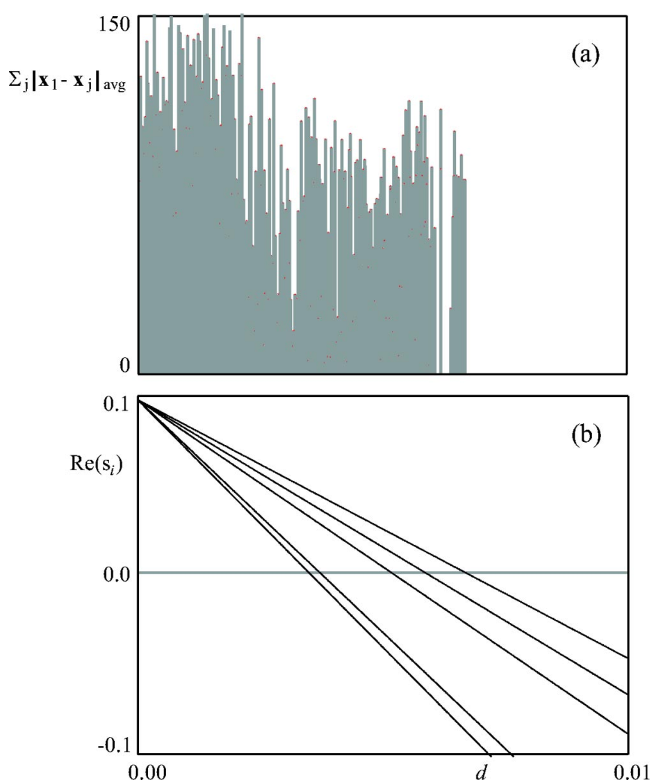

FIG. 7. Bifurcation diagram of average *trajectories separations* vs coupling coefficient (a) and corresponding eigenvalues of DSSM [Eq. (48)] (b) for ten Duffing oscillators with random structure of coupling [Eq. (47)].

IV. CONCLUSIONS

The presented theoretical analysis supported by numerical simulations leads to the main conclusion that chaotic synchronization in the networks composed of the identical oscillators with diagonal, diffusive-type interaction between them can be considered as simple, linear dynamical process. Two "parameters of order," i.e., the largest Lyapunov exponent of the network node system and the effective coupling rate between the nodes, play the dominant role in this process. This property of diagonal coupling allows us to estimate the synchronization threshold for arbitrary configuration of coupling. Such a method is based on the simplified, linear model of the network. The advantage of this approach is the simplicity of its application for both continuous-time and discrete-time systems. In order to examine the stability of the synchronization state, we introduce the concept of the *diffusive synchronization stability matrix*. The DSSM is constructed directly from a coupling configuration matrix and allows the linear stability analysis. The other advantage of the method is the possibility of application for node systems with discontinuities or time delay, if obviously we are able to estimate LLE of such a system. However, one should note that our approach can be realized only in the case of diagonal coupling because only in such a case can we substitute the coupling matrices for coupling coefficients according to Eq. (5). Nondiagonal coupling (realized by not all system coordinates for each pair of nodes) forces us to take the full mathematical form of the node system into consideration in the network synchronization process, which makes simplification of the network given by Eqs. (4) and (5) impossible. In such cases, other techniques for the determination of the synchronization condition have to be used, for instance the previously mentioned MSF. We would like to point out that the presented approach can be qualified as a version of the MSF method, but its possibilities of use in very different systems (maps and flows) makes it widely useful. However, we want to stress that the results have been obtained in a different way from the MSF. In the Appendix, we present the synchronization criteria analogous to inequalities (12) and (19) but derived on the basis of the MSF for diagonal coupling. The comparison of both approaches confirms the above conclusion that the method based on the DSSM can be treated as the version of MSF for the case of diagonal coupling.

ACKNOWLEDGMENT

This study has been supported by the Polish Committee for Scientific Research (KBN) under Project No. 5 T07A 014 23.

APPENDIX A: MASTER STABILITY FUNCTION FOR THE SYSTEMS WITH DIAGONAL COUPLING

We apply the idea of *master stability functions* [21,22] for the case when the coupling between nodes is diagonal. It will follow that only the largest Lyapunov exponent of the node system and eigenvalues of the coupling matrix are relevant for complete synchronization.

1. Time-continuous systems

Consider the system of coupled oscillators (nodes) of the form

$$\dot{\mathbf{x}}_i = \mathbf{f}(\mathbf{x}_i) + \sum_{r=1}^{n} G_{ij}\mathbf{H}(\mathbf{x}_j), \tag{A1}$$

where $j=1,2,\ldots,N$. The dynamics of the individual node is described, respectively, by

$$\dot{\mathbf{x}}_i = \mathbf{f}(\mathbf{x}_i). \tag{A2}$$

Here $\mathbf{x}_i \in \mathbb{R}^m$ is an m-dimensional vector of variables for each node, $i=1,2,\ldots,N$. We assume the function of the node's variables $\mathbf{H}(\mathbf{x})$, which is used in the coupling, is of the form $\mathbf{H}(\mathbf{x})=\mathbf{x}$, which indicates the diagonal linear coupling. The matrix of coupling coefficients $\{G_{ij}\}$ satisfies $\sum_{j=1}^{N} G_{ij}=0$ so that the synchronization manifold $\mathbf{x}_1=\cdots=\mathbf{x}_N$ is invariant.

Following [21,22], the system [Eq. (A1)] can be written in the form

$$\dot{\mathbf{x}} = \mathbf{F}(\mathbf{x}) + (\mathbf{G} \otimes I_m)\mathbf{x}, \tag{A3}$$

where $\mathbf{x}=(\mathbf{x}_1=\ldots=\mathbf{x}_N)$, $\mathbf{F}(\mathbf{x})=\mathbf{f}(\mathbf{x}_1),\ldots,\mathbf{f}(\mathbf{x}_N)$, and $\otimes$ is the direct (Kronecker) product of two matrices. Let $\mathbf{x}_1(t)=\cdots=\mathbf{x}_N(t)=\mathbf{s}(t)$ be a completely synchronous solution, satisfying $\dot{\mathbf{s}}=\mathbf{f}(\mathbf{s})$, and let $\xi_i \in \mathbb{R}^m$ be the variation of the ith node around this solution. Then for the collection of variations $\xi=(\xi_1,\ldots,\xi_N)$ we have

$$\dot{\xi} = [I_N \otimes D\mathbf{F}(\mathbf{s}(t)) + (\mathbf{G} \otimes I_m)]\xi, \tag{A4}$$

where I_N and I_m are unit matrices of size $N\times N$ and $m\times m$, respectively. The system [Eq. (A4)] can be block diagonalized with the blocks, cf. [21,22],

$$\dot{\eta}_k = [D\mathbf{F}(\mathbf{s}) + \gamma_k]\eta_k, \tag{A5}$$

where $\eta_k \in \mathbb{R}^m$ are new variations and γ_k are eigenvalues of the coupling matrix $\mathbf{G}$. Equation (A5) can be transformed into the system

$$\dot{\eta} = [D\mathbf{F}(\mathbf{s})]\eta \tag{A6}$$

by the change of variables $\eta_k \rightarrow \eta \exp(\gamma_k t)$. Since the system [Eq. (A6)] describes the variations for uncoupled oscillators and is characterized by the maximal Lyapunov exponent λ_1, then the variations in Eq. (A5) will be described by the transverse Lyapunov exponent $\lambda_1+\gamma_k$. If the real part of $\lambda_1+\gamma_k$ is negative, then the completely synchronous motion $\mathbf{s}(t)$ will be stable transversely. Therefore, the condition

$$\lambda_1 + \mathrm{Re}\ \gamma < 0 \tag{A7}$$

can serve as a simple criterion for the complete synchronization of the system [Eq. (A1)] of coupled oscillators. Here λ_1 is the maximal Lyapunov exponent of the uncoupled system [Eq. (A2)] and γ is the eigenvalue of the coupling matrix $\mathbf{G}$ with maximal real part (one zero eigenvalue, corresponding to the motion along the synchronization manifold, must be excluded).

2. Maps

The previous analysis can be generalized for the case of coupled maps,

$$\mathbf{x}_{n+1}^{i} = \mathbf{f}(\mathbf{x}_n^{i}) + \sum_{j=1}^{n} G_{ij}\mathbf{f}(\mathbf{x}_n^{j}), \tag{A8}$$

where $i,j=1,2,\ldots,N$. The dynamics of the individual node is described, respectively, by

$$\mathbf{x}_{n+1}^{i} = \mathbf{f}(\mathbf{x}_n^{i}). \tag{A9}$$

The matrix of coupling coefficients $\{G_{ij}\}$ satisfies $\sum_{j=1}^{N} G_{ij}=0$. Let $\xi^i \in \mathbb{R}^m$ be the variation of the ith node around the completely synchronous solution $\mathbf{x}_n^1=\cdots=\mathbf{x}_n^N=\mathbf{s}_n$. Then, for the collection of variations $\xi=(\xi^1,\ldots,\xi^N)$, we have

$$\xi_{n+1} = [I_N \otimes D\mathbf{F}(\mathbf{s}_n) + \mathbf{G} \otimes D\mathbf{F}(\mathbf{s}_n)]\xi_n. \tag{A10}$$

The system [Eq. (A10)] can be block diagonalized with the blocks

$$\eta_{n+1}^{k} = D\mathbf{F}(\mathbf{s}_n)[1+\gamma_k]\eta_n^{k}, \tag{A11}$$

where $\eta^k \in \mathbb{R}^m$ are new variations and γ_k are eigenvalues of the coupling matrix $\mathbf{G}$. It is clear that the stability of the zero fixed point of Eq. (A11) is characterized by the maximal Lyapunov exponent λ, which is related to the corresponding quantity λ_1 for the equation

$$\eta_{n+1} = [D\mathbf{F}(\mathbf{s}_n)]\ \eta_n \tag{A12}$$

as follows: $\lambda=\lambda_1(1+\gamma_k)$. As a result, the stability condition for a transverse mode is

$$\lambda_1|(1+\gamma)| < 1, \tag{A13}$$

where λ_1 is a maximal Lyapunov exponent of the uncoupled system [Eq. (A12)] and γ is an eigenvalue of the coupling matrix $\mathbf{G}$. In order to achieve the complete synchronization, inequality (A13) must be satisfied for all eigenvalues γ of the matrix $\mathbf{G}$, except one $\gamma=0$, which corresponds to the motion within the synchronization manifold. (Of course, additional zeros $\gamma=0$ can appear also in the transverse direction.)

[1] V. S. Afraimovich, N. N. Verichev, and M. Rabinovich, Izv. Vyssh. Uchebn. Zaved., Radiofiz. **28**, 1050 (1985).
[2] I. Blekhman, P. S. Landa, and M. G. Rosenblum, Appl. Mech. Rev. **48**, 733 (1995).
[3] R. Brown, H. F. Rulkov, and N. B. Tufillaro, Phys. Lett. A **196**, 201 (1994).
[4] H. Fujisaka and T. Yamada, Prog. Theor. Phys. **69**, 32 (1983).
[5] T. Yamada and H. Fujisaka, Prog. Theor. Phys. **70**, 1240 (1983).
[6] T. Kapitaniak, Phys. Rev. E **50**, 1642 (1994).
[7] T. Kapitaniak, M. Sekieta, and M. Ogorzałek, Int. J. Bifurcation Chaos Appl. Sci. Eng. **6**, 211 (1996).
[8] Y. Maistrenko and T. Kapitaniak, Phys. Rev. E **54**, 3285 (1996).
[9] L. M. Pecora and T. L. Carroll, Phys. Rev. Lett. **64**, 821 (1990).
[10] L. M. Pecora and T. L. Carroll, Phys. Rev. A **44**, 2374 (1991).
[11] A. Pikovsky, Z. Phys. B: Condens. Matter **55**, 149 (1984).
[12] A. Pikovsky and P. Grassberger, J. Phys. A **24**, 4587 (1991).
[13] K. Pyragas, Phys. Lett. A **181**, 203 (1993).
[14] A. Stefański and T. Kapitaniak, Int. J. Solids Struct. **40**, 5175 (2003).
[15] R. Brown and N. F. Rulkov, Phys. Rev. Lett. **78**, 4189 (1997).
[16] A. S. Dmitriev, M. Shirokov, and S. O. Starkov, IEEE Trans. Circuits Syst., I: Fundam. Theory Appl. **44**, 918 (1997).
[17] P. M. Gade, Phys. Rev. E **54**, 64 (1996).
[18] P. M. Gade, H. Cerdeira, and R. Ramaswamy, Phys. Rev. E **52**, 2478 (1991).
[19] J. F. Heagy, T. L. Carroll, and L. M. Pecora, Phys. Rev. E **50**, 1874 (1994).
[20] Y. Kuramoto, in *International Symposium on Mathematical Problems in Theoretical Physics*, edited by H. Araki (Springer, Berlin, 1975), p. 420.
[21] L. M. Pecora and T. L. Carroll, Phys. Rev. Lett. **80**, 2109 (1998).
[22] L. M. Pecora, T. L. Carroll, G. Johnson, D. Mar, and K. Fink, Int. J. Bifurcation Chaos Appl. Sci. Eng. **10**, 273 (2000).
[23] C. W. Wu, *IEEE International Symposium on Circuits and Systems, Monterey, CA* (IEEE Press, Piscataway, NJ, 1998), p. 302.
[24] C. W. Wu and L. O. Chua, Int. J. Bifurcation Chaos Appl. Sci. Eng. **4**, 979 (1994).
[25] C. W. Wu and L. O. Chua, IEEE Trans. Circuits Syst., I: Fundam. Theory Appl. **42**, 430 (1995).
[26] D. Watts and S. H. Stroganz, Nature (London) **393**, 440 (1998).
[27] X. F. Wang and G. Chen, Int. J. Bifurcation Chaos Appl. Sci. Eng. **12**, 273 (2002).
[28] W. T. Vetterling, S. A. Teukolsky, H. Press, and B. P. Flannery, *Numerical Recipes in C: The Art of Scientific Computing* (Cambridge University Press, Cambridge, 1992).